



Contents lists available at ScienceDirect

Tetrahedron Letters

journal homepage: www.elsevier.com/locate/tetlet

Electrodeposited palladium on MWCNTs as ‘semi-soluble heterogeneous’ catalyst for cross-coupling reactions

Mariusz Radtke^a, Steffi Stumpf^{b,d}, Bernd Schröter^c, Stephanie Höppener^{b,d}, Ulrich Sigmar Schubert^{b,d}, Anna Ignaszak^{a,*}

^a Institute of Organic and Macromolecular Chemistry, Friedrich-Schiller-University, Lessingstrasse 12, 07743 Jena, Germany

^b Institute of Organic and Macromolecular Chemistry, Friedrich-Schiller-University, Philosophenweg 7, 07743 Jena, Germany

^c Institute of Solid State Physics, Friedrich-Schiller University, Philosophenweg 7, 07743 Jena, Germany

^d Jena Center of Soft Mater (JCSM), Friedrich-Schiller University, Philosophenweg 7, 07743 Jena, Germany

ARTICLE INFO

Article history:

Received 9 April 2015

Revised 1 May 2015

Accepted 6 May 2015

Available online xxxxx

Keywords:

Electrodeposited nanoparticles

Cross coupling

Suzuki–Miyaura reaction

Sonogashira reaction

Buchwald–Hartwig reaction

ABSTRACT

Platinum group metals (PGM) catalyze many important chemical processes including hydrogenation; electro-catalysis applied to fuel cell and battery technologies and one of the most prominent the C_{sp2} – C_{sp2} cross-coupling reactions such as Sonogashira, Suzuki–Miyaura, and C_{sp2} – N_{sp3} cross-coupling as for the Buchwald–Hartwig type reactions.

The main concern of the catalytic reaction is the recovery and recyclability of used catalytic entities. Recent efforts in the catalyst fabrication focus on combining a nano-sized metal with various high surface area supports like resins or carbon-based materials that allow recovering the catalyst after each reaction in a simple and convenient way. This work aims to investigate the catalytic activity of the carbon-supported (MWCNTs) electrodeposited metallic nanoparticles (Pd) and their applications in several cross-coupling reactions. We propose a simple and affordable synthesis of the high surface area Pd–C composite that can be re-used until deactivated. The intramolecular interactions between carbon and metallic fractions studied by X-ray photoelectron spectroscopy are discussed with respect to the catalytic efficiencies.

© 2015 Elsevier Ltd. All rights reserved.

Introduction

Pd catalysis is very versatile and has broad application in the synthesis of natural products, agrochemicals, pharmaceuticals, and polymers that involve the cross coupling chemistry including the Suzuki–Miyaura,¹ a copper-free Sonogashira reaction,² and C_{sp2} – N_{sp3} coupling Buchwald–Hartwig reactions.³ There are still several challenges behind, one is the cost and availability of Pd precursors and the second is a recovery of the Pd catalyst and the problem of contamination by a residual Pd and ligands that are difficult to separate from the product.⁴ As the solution, the promising approach is to immobilize the catalyst onto various supports from which the carbon-based materials are the most suitable.⁵ Such reusable heterogeneous Pd–carbon systems allow recovering the catalyst in a convenient way after each reaction, as for the Pd/C-catalyzed Suzuki–Miyaura couplings.⁶ Regarding the environmental aspect, this will contribute to the minimization of chemical waste release/disposal that is always a serious issue in a large-scale

production (e.g., to minimize the contamination by Pd and ligands that are difficult to separate from the synthesis mixture). In addition, the catalyst utilization while maintaining or improving the catalytic efficiency is an important task. This is usually accomplished by generating the nano-sized catalyst particles or by dispersing the nanocatalyst on a high surface area support, such as graphene oxide.⁷ This combination generates a very large catalytic interphase that significantly enhances the process efficacy at lower overall cost of the catalyst in comparison to the commercial Pd-complex type catalysts such as $Pd(OAc)_2$.⁷

One of the most promising, affordable, and non-toxic support is carbon. Regardless of the price, carbon is chemically inert and can be synthesized with desired porosity and surface functionalization. For this particular application (organic cross-coupling), carbon nanotubes are of special interest since their morphology promotes a fast mass transport to the catalytic active sites.⁸ The disadvantage of carbon is its low dispersibility. In order to overcome this limitation, various surface functionalizations are offered to control the hydrophilic/hydrophobic balance, depending on the application requirement.⁹ One of the biggest challenge for the heterogeneous catalyst (also called ‘semi-soluble’ due to the presence of soluble

* Corresponding author. Tel./fax: +49 (0)36 41 94 8290.

E-mail address: anna.ignaszak@uni-jena.de (A. Ignaszak).

Pd and insoluble carbon) is to maintain (or exceed) the solubility that should be comparable to the homogenous analog (Pd) or better.⁹ In this work we will introduce soluble Pd nanoparticles into the carbon matrix in order to deliver a long-life and active system with an expanded catalytic interface. This will be accomplished by homogenous dispersion of metal nano-objects onto high surface area carbon resulting in continuous release of Pd (and re-deposition).

With respect to the synthesis methods of the active metal cluster supported (or not) on carbon, a well-known one is the conventional reduction of the metal cation by a strong reducing agent such as borohydride,¹⁰ ascorbic acid¹¹ or polyol methods in organic phase,¹² also in the presence of organic surfactants (e.g., PVP, CTAB).^{13a} All listed fabrication pathways offer a nano-size

product but necessitate using toxic chemicals or high temperature,^{13b} followed by a time-consuming washing process (usually viscous solvents/surfactants are involved). To address these, the electrodeposition of metal seems to be a good alternative.¹⁴ One of the biggest advantages of this approach—often classified as a ‘green chemistry method’¹⁵—is processing at ambient conditions while using the aqueous inorganic precursors. This electro-synthesis is very fast and easy to scale up at low cost. There are several modes of Pd plating, some involve scanning the potential in the required range,¹⁰ the galvanostatic mode is carried out at constant current¹⁴ or at constant potential¹⁵ from a solution of Pd inorganic salts (e.g., PdCl₂). An interesting one is the simultaneous deposition of carbon and metal carried out by applying the charge or potential to the conductive surface (working electrode) immersed in the solution composed of the metal salt, carbon, and electrolyte (e.g., 1 M KCl). The working electrode (glassy carbon plate, Ni mesh) acts as the scavenger of the carbon-reinforced metal particles.^{16,17}

The particle size and the metal load on carbon is usually controlled by the concentration of the deposition solution¹⁸ or the electrochemical parameters (time, deposition potential, or current).¹⁵

In this study we aim to generate the Pd–carbon nanotube semi-soluble catalyst using electrodeposition methods at ambient conditions. The intramolecular metal–carbon interactions will be examined by X-ray photoelectron spectroscopy and discussed with respect to the catalyst efficiencies for selected cross-check coupling reactions: Sonogashira, Suzuki–Miyaura, and Buchwald–Hartwig type reactions.

Results and discussion

Figure 1 represents cyclic voltammogram of the Pd electrodeposition from the aqueous solution of PdCl₂ onto the glassy carbon electrode. The potential scan reveals the Pd metal deposition at 0.23 V via an electrochemical reduction of the Pd²⁺ ($\text{Pd}^{2+} + 2\text{e}^- \rightarrow \text{Pd}^0$) followed by the electrochemical dissolution (anodic stripping) of the metal deposit at 0.93 V ($\text{Pd}^0 \rightarrow \text{Pd}^{2+} + 2\text{e}^-$).¹⁶ The deposition and the stripping peaks of Pd are slightly smaller for the first CV scan when comparing to the final voltammogram, which is associated with the nucleation process and the dissolution rate of the

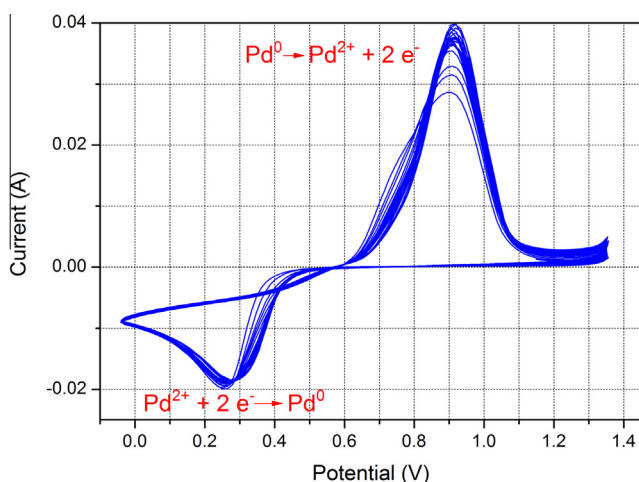


Figure 1. Cyclic voltammogram of Pd electrodeposition on multi walled carbon nanotubes from PdCl₂ aqueous solution.

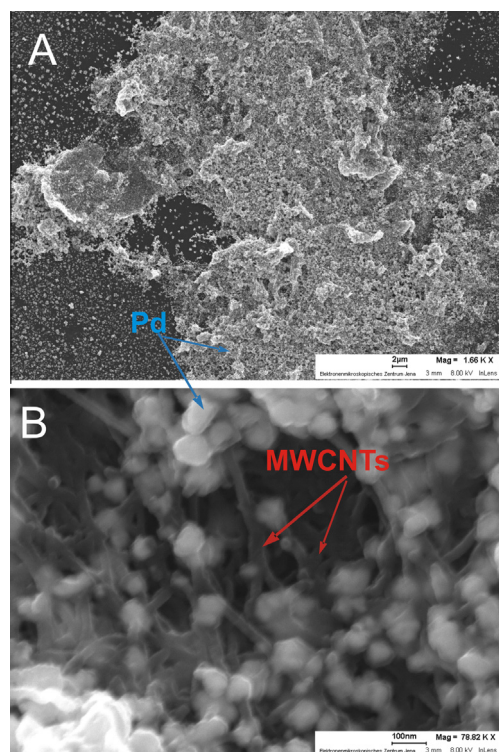


Figure 2. SEM image of the as-prepared Pd@MWCNT catalyst.

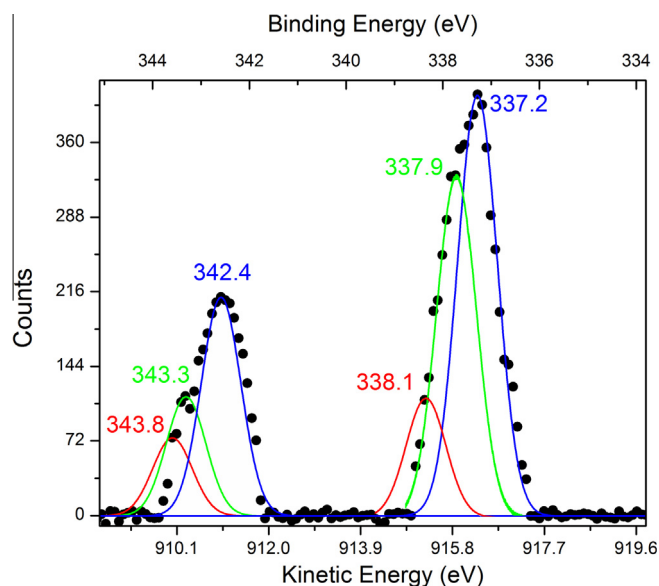
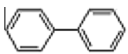
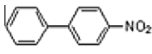

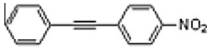
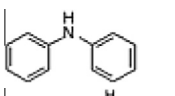
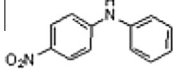


Figure 3. XPS Pd 3d narrow scan of Pd@MWCNT catalyst.

Table 1
Yields of the cross-coupling reactions catalyzed by Pd@MWCNTs

Reaction type	Yields ^a (after 1 st /2 nd /3 rd use)	
Suzuki–Miyaura ^b	84/62/31	
	87/50/41	
Sonogashira ^b	71/42/12	
	78/51/10	
Buchwald–Hartwig ^c	9/0/0	
	0/0/0	

^a With respect to the phenyl iodide/4-nitro iodobenzene.

^b Experimental conditions: aerobic atmosphere, reflux, 2.5 h, MeOH/H₂O 3:1.

^c Experimental conditions: nitrogen atmosphere, 110 °C, 16 h, MeOH/H₂O 3:1.

deposited metal. Pd seeds generated in first scan act as nucleation centers for the following deposition, resulting in slightly higher peak current at 0.23 V. Also, an interesting observation is that the

stripping peak is larger than the corresponding reduction counterpart and is correlated with the formation of palladium complexes.¹⁶ The peak separation ($\Delta E_{a-c} > 60$ mV) indicates that the redox system is irreversible due to the complexity (multistep deposition¹⁶) and a residual metal crystallization on the electrode surface.¹⁰

Figure 2 shows the SEM image at low (A) and high magnification (B) as-prepared Pd@MWCNTs catalysts. The metal particles with uniform spherical shape and size in the range from 30 to 70 nm are evenly distributed on carbon. Figure 2B reveals a very homogenous metal deposit generated during a three-dimensional Pd growth, resulting in interconnected structures with a superior surface area. The Pd-to-carbon weight ratio was 1:263 as estimated electrochemically according to the Faraday law (details of this analysis are provided in Supporting information).

Figure 3 represents XPS narrow scan of Pd 3d signal of the Pd@MWCNTs revealing the most important chemical states of the metal. The core-level Pd 3d spectrum is composed of three doublets (3d_{5/2} signals at lower BE and 3d_{3/2} at higher BE, respectively). The binding energies of 337.6 eV and 342.4 eV represent Pd⁰, at 337.9 and 343.3 eV are assigned to Pd²⁺ species (e.g., oxidized metal, PdO), a high-BE doublet with peaks at 338.1 and 343.8 eV represents palladium complexes (can be generated during the reaction with supporting electrolyte: PdCl₂ + 2KCl → K₂PdCl₄) or Pd species at higher oxidation state.¹⁹

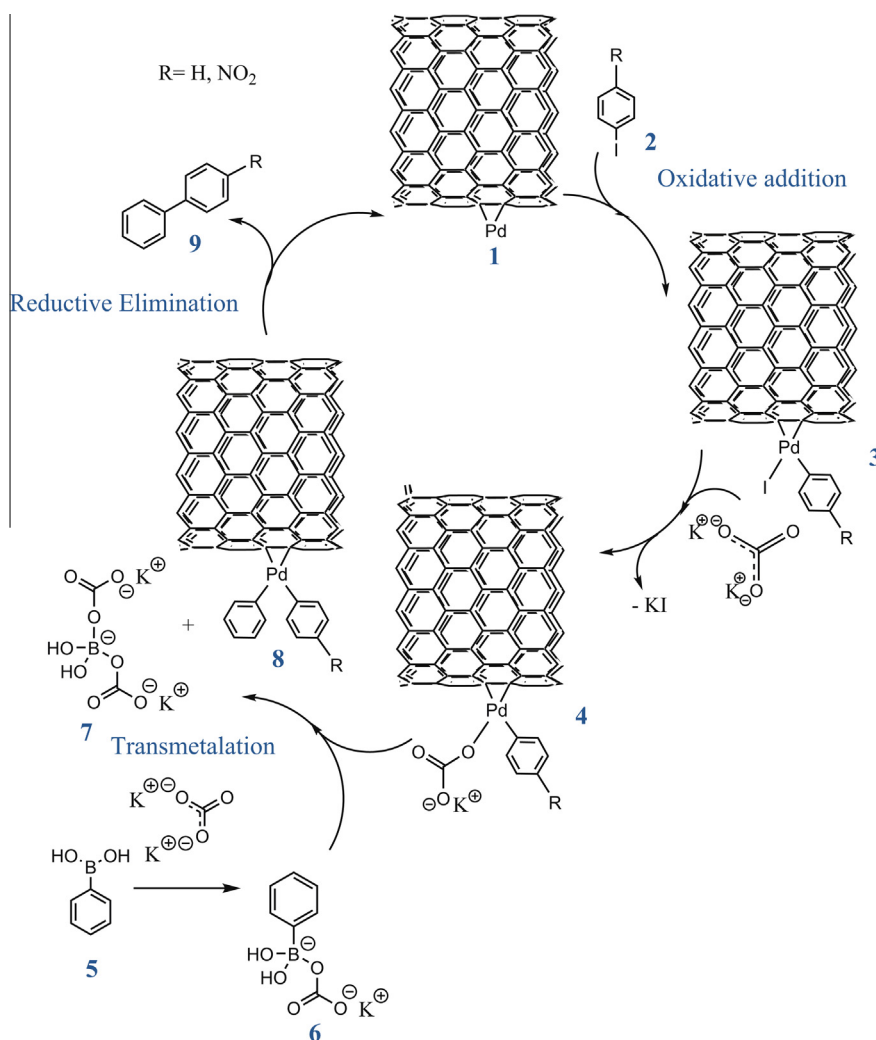


Figure 4. Proposed mechanism for Suzuki reaction based on Pd@MWCNT catalyst.

Pd⁰ signals are slightly shifted toward higher binding energy, which is associated with strong electronic interactions between the metal and MWCNTs.²⁰ Such an effect originates from the electron rearrangement between the C and Pd atoms, resulting in the formation of interface states (this is also associated with the depletion of electrons at the metal–carbon and outer metal surface. This electron shift at the Pd–CNTs contact is even stronger for a highly functionalized carbon surface, as it is in our case.²¹ The XPS C 1s narrow scan (Fig. S1, Supporting information) shows the high level of MWCNTs functionalization that contributes in the observed BE shift for Pd lines and is included in Supplementary materials.

Suzuki–Miyaura, Sonogashira, Buchwald–Hartwig coupling

In order to validate the catalytic activity of Pd@MWCNTs we carried out several cross-coupling reactions with the Pd/MWCNT system. Table 1 summarizes efficiencies of the coupling reactions obtained in this work.

Figure 4 represents an example of the proposed mechanism for synthetic cycle of Suzuki reaction catalyzed by Pd@MWCNTs. In this process the following standard steps for homo/cross-coupling are projected: in the first phase an oxidative addition between aryl halide and aryl boronic followed by the sub-sequential first transmetalation with potassium carbonate leading to transmetalation with aryl borate. The coupling product is generated in the last step via reductive elimination. It is important to notice that dehalogenated products were not identified.

With respect to yields accomplished for the Suzuki–Miyaura, the catalytic efficiency of Pd@MWCNTs is very close to the same reaction catalyzed by Pd black¹ or Pd–C.⁹ Regarding the Sonogashira reaction, yields are smaller than reported in the literature.^{22,13b} Based on this observation we conclude that Pd@MWCNTs is as good or even outperforms (for some cross-couplings) the conventional catalyst and can be an excellent competitor for the commercial expensive metal blacks. An interesting result was observed for the Pd@MWCNTs-catalyzed Buchwald–Hartwig reaction. Since the yields are very low, we predict that in this particular case lack of electron-rich ligands makes this heterogeneous catalyst inactive (the reactive 14e[−] Pd complex was not generated²³).

Activity of the catalyst after second and third cycle drops due to the dissolution of metallic nanoparticles during the reaction (Fig. S2 provided in the Supporting information). The yields of reactions and their selectivity are in good agreement with those reported in the literature.^{9,16,24}

Conclusions

In this work we offer the electro-synthesized Pd nanocatalyst decorated onto a high surface area carbon. This system revealed a very good catalytic activity toward the Suzuki–Miyaura and Sonogashira cross-coupling reactions generating the product in yields comparable to that catalyzed by a commercial Pd black. The heterogeneous catalyst generated in this work shows high selectivity since homo-coupling products potentially generated during the reaction of phenyl acetylene and 1-iodo-4-nitrobenzene were not identified. In contrast, the catalytic efficiency for the

Buchwald–Hartwig amination was very poor, revealing that at operating conditions the electron-rich reactive ligands were not generated. The catalyst recovered after the (homo)cross-coupling reaction was repeatedly used until deactivated due to the partial dissolution of Pd or phase separation in Pd@MWCNTs. The stronger catalyst–support interaction can be the way of improvement of the heterogeneous catalyst reusability—this can be done by adapting new carbon allotropes and will be the subject of future work. The scope of this study will be extended by application of the heterogeneous catalyst in the synthesis of bioactive natural products with cooperation of FSU IOMC Jena.

Acknowledgments

We thank Carl-Zeiss Foundation Germany for the financial support. Cryo-TEM investigations were performed at the cryo-TEM facilities of the Jena Center for Soft Matter (JCSM). TEM facilities were funded by a grant of the DFG (German Research Foundation) and the EFRE (European Fund for Regional Development).

Supplementary data

Supplementary data associated with this article can be found, in the online version, at <http://dx.doi.org/10.1016/j.tetlet.2015.05.019>.

References and notes

- Miyaura, N.; Suzuki, A. *Chem. Rev.* **1995**, *95*, 2457–2483.
- Méry, D.; Heuzé, K.; Astruc, D. *Chem. Commun.* **2003**, 1934–1935.
- Paul, F.; Patt, J.; Hartwig, J. F. *J. Am. Chem. Soc.* **1994**, *116*, 5969–5970.
- Karami, K.; Ghasemi, M.; Naeini, N. H. *Catal. Commun.* **2013**, *38*, 10–15.
- Seki, M. *Synthesis* **2006**, *18*, 2975–2992.
- Kitamura, Y.; Sakurai, A.; Udzu, T.; Maegawa, T.; Monguchi, Y.; Sajiki, H. *Tetrahedron* **2007**, *63*, 10596–10602.
- Shendage, S. S.; Singh, A. S.; Nagarkar, J. M. *Tetrahedron Lett.* **2014**, *22*, 857–860.
- Cornelio, B.; Rance, G. A.; Cochar, M. L.; Fontana, A.; Sapi, J.; Khlobystov, A. N. *J. Mater. Chem. A* **2013**, *1*, 8737–8744.
- Guerra, J.; Herrero, M. A. *Nanoscale* **2010**, *2*, 1390–1400.
- Ma, J.; Sahai, Y.; Buchheit, R. G. *J. Power Sources* **2010**, *195*, 4709–4713.
- Yan, J.; Liu, S.; Zhang, Z.; He, G.; Zhou, P.; Liang, H.; Tian, L.; Zhou, X.; Jiang, H. *Colloids Surf., B* **2013**, *111*, 392–397.
- Tsuji, M.; Miyamae, N.; Hashimoto, M.; Nishio, M.; Hikino, S.; Ishigami, N.; Tanaka, I. *Colloids Surf., A* **2007**, *302*, 587–598.
- (a) Wang, S.; Li, Y.; Wang, Y.; Yang, Q.; Wei, Y. *Mater. Lett.* **2007**, *61*, 4674–4678; (b) Olivier, J.-H.; Camerel, F.; Ziessel, R.; Retailleau, P.; Amadou, J.; Pham-Huu, C. *New J. Chem.* **2008**, *32*, 920–924.
- Kim, K. T.; Jin, S.-H.; Chang, S.-C.; Park, D.-S. *Bull. Korean Chem. Soc.* **2013**, *34*, 3835–3839.
- Reetz, M. T.; Helbig, W. *J. Am. Chem. Soc.* **1994**, *116*, 7401–7402.
- Shendage, S. S.; Singh, A. S.; Nagarkar, J. M. *Tetrahedron Lett.* **2014**, *55*, 857–860.
- Al Abass, A. A.; Denuault, G.; Pletcher, D. *Phys. Chem. Chem. Phys.* **2014**, *16*, 4892–4899.
- Hirsch, T.; Zharnikov, M.; Shaporenko, A.; Stahl, J.; Weiss, D.; Wolfbeis, O. S.; Mirsky, V. M. *Angew. Chem., Int. Ed.* **2005**, *44*, 6775–6778.
- Lisowski, W.; Keim, E. G. *Anal. Bioanal. Chem.* **2010**, *396*, 2797–2804.
- Zhu, W.; Kaxiras, E. *Phys. Stat. Sol.* **2006**, *243*, 2164–2169.
- Adjizian, J. J.; De Marco, P.; Suarez-Martinez, I.; El Mel, A. A.; Snyders, R.; Gengler, R. Y. N.; Rudolf, P.; Ke, X.; Van Tendeloo, G.; Bittencourt, C.; Ewels, C. P. *Chem. Phys. Lett.* **2013**, *571*, 44–48.
- Bakherad, M.; Keivanloo, A.; Kalantar, Z.; Jajarmi, S. *Tetrahedron Lett.* **2011**, *52*, 228–230.
- Wolfe, J.; Wagaw, S.; Buchwald, S. J. *J. Am. Chem. Soc.* **1996**, *118*, 7215–7216.
- Khairmar, B. J.; Dey, S.; Jain, V. K.; Bhanage, B. M. *Tetrahedron Lett.* **2014**, *55*, 716–719.